



## Seasonal and interannual relations between precipitation, surface soil moisture and vegetation dynamics in the North American monsoon region

Luis A. Méndez-Barroso<sup>a</sup>, Enrique R. Vivoni<sup>a,b,d,\*</sup>, Christopher J. Watts<sup>b</sup>, Julio C. Rodríguez<sup>c</sup>

<sup>a</sup> Department of Earth and Environmental Science, New Mexico Institute of Mining and Technology, Socorro, NM 87801, United States

<sup>b</sup> Departamento de Física, Universidad de Sonora, Hermosillo, Sonora, México 83100, Mexico

<sup>c</sup> Departamento de Agricultura y Ganadería, Universidad de Sonora, Hermosillo, Sonora, México 83100, Mexico

<sup>d</sup> School of Earth and Space Exploration and School of Sustainable Engineering and the Built Environment, Arizona State University, Tempe, AZ 85287, United States

### ARTICLE INFO

#### Article history:

Received 1 May 2009

Received in revised form 28 June 2009

Accepted 2 August 2009

This manuscript was handled by K. Georgakakos, Editor-in-Chief, with the assistance of Phillip Arkin, Associate Editor

#### Keywords:

North American monsoon  
Semi-arid ecosystems  
Ecohydrology  
Remote sensing  
Spatiotemporal variability  
Watershed

### SUMMARY

The North American monsoon (NAM) region in northwestern Mexico is characterized by seasonal precipitation during the summer that leads to a major shift in ecosystem processes. Seasonal greening in the semi-arid region is important due to its impact on land surface conditions and its potential feedback to atmospheric and hydrologic processes. In this study, we analyzed vegetation dynamics using remotely-sensed Enhanced Vegetation Index (EVI) images over the period 2004–2006 for the Río San Miguel and Río Sonora basins, which contain a regional network of precipitation and soil moisture observations. Results indicate that changes in vegetation greenness are dramatic for all ecosystems and are directly related to differences in hydrologic conditions. Vegetation responses depend strongly on the plant communities, with the highest greening occurring in mid-elevation Sinaloan thornscrub, which also exhibited the largest greenness–precipitation ratio (GPR), a measure of the plant capacity to convert precipitation into biomass. Analyses of the spatial and temporal persistence of EVI fields are used to distinguish the spatial organization of the vegetation response during the NAM. Correlation of vegetation greenness and accumulated monthly precipitation increased with the number of preceding months, while the correlation between greenness and surface soil moisture was equal to that of precipitation for the current month and lower than precipitation for longer lagged periods. Comparisons across ecosystems indicate that different plant water use strategies exist in response to hydrologic variations and are strongly controlled by elevation along semi-arid mountain fronts.

© 2009 Elsevier B.V. All rights reserved.

### Introduction

The ecohydrology of northwestern Mexico is marked by ecosystem responses to precipitation during the North American monsoon (NAM), which accounts for ~60–75% of the annual rainfall in the region (Douglas et al., 1993). Plant responses during the NAM include the production of biomass required for photosynthesis, flowering and seed dispersal (e.g., Reynolds et al., 2004; Weiss et al., 2004; Caso et al., 2007). The vegetation transition from leaf-off to leaf-on conditions occurs relatively rapidly and is closely tied to the NAM onset time and its interannual variability. While this has been recognized previously (e.g., Brown, 1994; Salinas-Zavala et al., 2002), the direct linkage between hydrologic conditions and ecosystem responses has not been quantified, primarily due

to a lack of regional observations. Fortunately, the scarcity of field data has been recently addressed through the North American Monsoon Experiment and the Soil Moisture Experiment in 2004 (SMEX04-NAME) (Higgins and Gochis, 2007; Bindlish et al., 2008). As a result, an opportunity exists to relate hydrologic observations to vegetation estimates derived from remote sensing products (e.g., Vivoni et al., 2008a).

Satellite remote sensing has become an important tool for vegetation monitoring (e.g., Xinmei et al., 1993; Guillevic et al., 2002; Bounoua et al., 2000; Wang et al., 2006). For example, the Normalized Difference Vegetation Index (NDVI) has been used widely to estimate changes in plant greenness (Sellers, 1985; Tucker et al., 1985; Goward, 1989; Zhang et al., 2003). NDVI is based on the reflection properties of green vegetation and is determined by the ratio of the amount of absorption by chlorophyll in the red wavelength (600–700 nm) to the reflectance of the near infrared (720–1300 nm) radiation. To improve upon NDVI, the Enhanced Vegetation Index (EVI) was developed for high biomass areas by de-coupling the canopy from the background signal and reducing

\* Corresponding author. Address: School of Earth and Space Exploration, Arizona State University, Bateman Physical Sciences Center F-Wing, Room 650-A, United States. Tel.: +1 480 965 5228; fax: +1 480 965 8102.

E-mail address: [vivoni@asu.edu](mailto:vivoni@asu.edu) (E.R. Vivoni).

atmospheric effects. The canopy background correction is particularly relevant for monitoring areas consisting of open canopies such as desert shrublands, grasslands and savannas (Huete et al., 1997).

One of the most reliable sources of remotely-sensed vegetation data is the MODIS (Moderate Resolution Imaging Spectroradiometer) sensor (Huete et al., 1997, 2002). MODIS products can indicate spatial and temporal variations in: (1) the onset of photosynthesis, (2) the peak photosynthetic activity, and (3) the senescence, mortality or removal of vegetation (e.g., Reed et al., 1994; Zhang et al., 2003). In prior studies, remote sensing of vegetation has yielded metrics useful for monitoring ecosystem changes (e.g., Lloyd, 1990; Reed et al., 1994; Zhang et al., 2003). An important contribution has been the time integrated NDVI (iNDVI), which is related to the net primary productivity (NPP) in an ecosystem (Reed et al., 1994). iNDVI measures the magnitude of greenness integrated over time and reflects the capacity of an ecosystem to support photosynthesis and biomass production. As a result, the relation between rainfall and iNDVI has been used as an indicator of ecosystem productivity. An analogous metric that integrates EVI in time (iEVI) can take advantage of the improved vegetation monitoring in semiarid regions achieved through this vegetation index.

In this study, we use MODIS-derived EVI fields to examine semiarid ecosystems in northwestern Mexico, which respond vigorously to summer rainfall during the NAM. EVI is preferred over the more traditional NDVI, as used in Salinas-Zavala et al. (2002), since most ecosystems have high background signals. Understanding vegetation dynamics and its relation to hydrologic conditions during the NAM is important as this period coincides with the major growing season (e.g., Watts et al., 2007; Vivoni et al., 2007, 2008b). We base our investigation on previous studies that have shown strong relations between precipitation and vegetation in other arid and semiarid areas (Prasad et al., 2005; Li et al., 2004; Wang et al., 2003; Chamaille-Jammes et al., 2006). Prior studies indicate that maximum photosynthetic activity is linked with precipitation in the current and preceding months. Although vegetation growth is correlated to rainfall, the soil water balance also plays a key intermediary role between seasonal storms and plant water uptake (Breshears and Barnes, 1999; Loik et al., 2004). As a result, quantifying the correlation between soil moisture and vegetation dynamics is also important. For water-limited ecosystems, the greenness–precipitation ratio (GPR), defined as the net primary productivity per unit rainfall, has been also used to quantify productivity (e.g., Davenport and Nicholson, 1993; Prasad et al., 2005). Quantifying the GPR in the NAM region would indicate the strength of the linkage between hydrologic conditions and the vegetation greening.

## Methods

### Study region and ecosystem distributions

The study region encompasses the Río San Miguel and Río Sonora basins in northwestern Mexico in Sonora (Fig. 1). The total area for both watersheds is ~15,842 km<sup>2</sup>. The analysis extends beyond the basin boundaries to cover an area of 53,269 km<sup>2</sup> including portions of the Río Yaqui and San Pedro River basins. The study region is characterized by complex terrain with north–south trending mountain ranges. The two major ephemeral flow rivers are Río San Miguel and Río Sonora, which run from north to south. Basin areas were delineated from a 29-m digital elevation model (DEM) using two stream gauging sites as outlet points (Fig. 1). For the Río San Miguel, the outlet is a gauging site managed by the Comisión Nacional del Agua (CNA) known as El Cajón (110.73°W; 29.47°N), while the Río Sonora was delineated with re-

spect to the El Oregano CNA gauge (110.70°W; 29.22°N). Elevation above sea level in the region fluctuates between 130 and 3000 m. Mean annual precipitation in the region varies approximately from 300 to 500 mm and is controlled by latitudinal position and elevation (Chen et al., 2002; Gochis et al., 2007). A wide variety of ecosystems are found in the study region due to the strong variations in elevation and climate over short distances (e.g., Brown, 1994; Salinas-Zavala et al., 2002; Coblenz and Riitters, 2004). Ecosystems are arranged along elevation gradients in the following fashion (from low to high elevation): Sonoran desert scrub, Sinaloan thornscrub, Sonoran riparian deciduous woodland, Sonoran savanna grassland, Madrean evergreen woodland and Madrean montane conifer forest (Brown, 1994). The reader is referred to Méndez-Barroso (2009) for specific details on the ecosystem characteristics.

### Field and remote sensing datasets

We selected a three-year period (2004–2006, with portions of 2007) to capture vegetation dynamics during monsoons exhibiting different rainfall amounts. Ground-based precipitation and soil moisture observations were obtained from a network of 15 sites installed during 2004 (Vivoni et al., 2007). Fig. 1 presents the locations of the stations, with five sites in the Río Sonora and 10 sites in the Río San Miguel. Table 1 presents the station locations, ecosystem classifications and elevations. Precipitation data (mm/h) were acquired with a 6-inch tipping bucket rain gauge (Texas Electronics, T5251), while volumetric soil moisture (% in hourly intervals) was obtained at a 5-cm depth with a 50-MHz soil dielectric sensor (Stevens Water Monitoring, Hydra Probe). The Hydra Probe determines soil moisture by making high frequency measurements of the complex dielectric constant. We used a factory calibration for sandy soils to transform the dielectric measurement to volumetric soil moisture (Seyfried and Murdock, 2004). Missing data exists during the study period due to equipment malfunction or site inaccessibility (see Méndez-Barroso (2009) for details). Hourly precipitation and soil moisture data were accumulated or averaged over the 16-day intervals to match the MODIS compositing period.

In this study, we utilize surface soil moisture measurements at 5 cm as representative of hydrologic conditions at each site. This depth was selected based on the instrument network design and its use for validating remote sensing data (Vivoni et al., 2007, 2008a). We found that surface moisture was well correlated with deeper soil moisture values (10 and 15 cm) at station 147 using data from 2004 to 2006 ( $r^2 = 0.68$  and  $r^2 = 0.71$ , respectively). This correlation was found to be strongest for concurrent periods at the daily time scale (not shown). The use of surface soil moisture to infer conditions in the entire profile is particularly relevant during dry periods because the variability in the soil moisture profile increases with wetter conditions (Martinez et al., 2008; Famiglietti et al., 1998; Mohanty et al., 2000; De Lannoy et al., 2006). These results are in agreement with Martinez et al. (2008), Mahmood and Hubbard (2007) and Calvet et al. (1998), who found that surface soil moisture is well correlated with root zone soil moisture (0–30 cm). For the shallow rooted plants in regional ecosystems, the surface moisture plays an important role in plant water uptake and evapotranspiration (e.g., Casper et al., 2003; Seyfried and Wilcox, 2006; Vivoni et al., 2008b). Nevertheless, the regional ecosystems are expected to have deeper roots, possibly up to 1.5 m, that also control plant water uptake, though 50% of the roots are expected in the top 30 cm (Schenk and Jackson, 2002).

MODIS EVI data were acquired from the EOS Data Gateway. Sixteen day composites of the 250-m EVI products from MODIS–Terra were obtained from January 2004 to June 2007 for a total of 83 images. MODIS–Terra overpasses the region around 11:00 AM local time (18:00 UTC). Each of the MODIS images was clipped, merged and reprojected using the HDF–EOS to GIS Format Conversion Tool

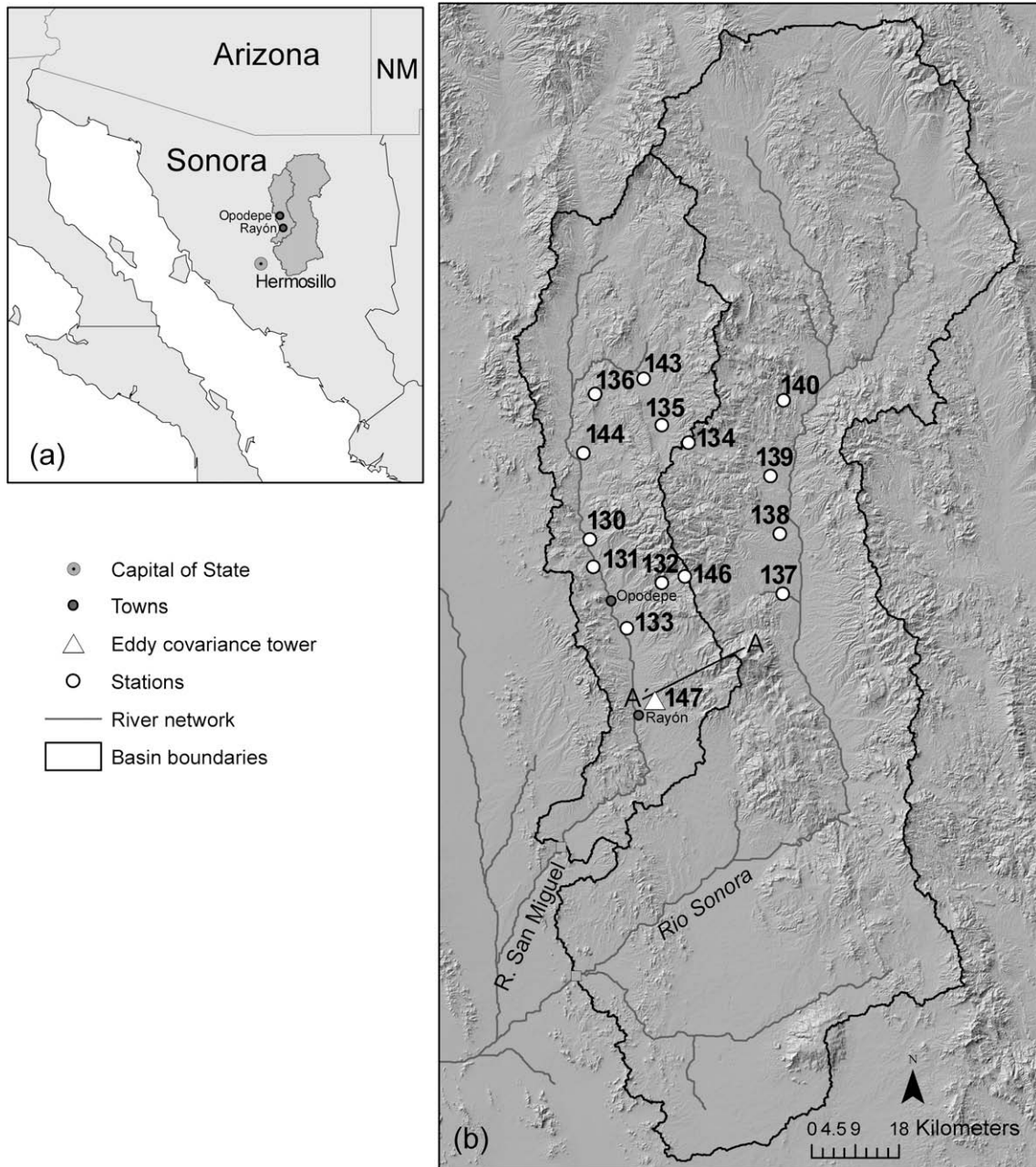


**Fig. 1.** (a) Regional map showing the location of the Río San Miguel (3798 km<sup>2</sup>) and Río Sonora (11,684 km<sup>2</sup>) basins in Sonora, Mexico. (b) Location of the regional stations with precipitation and soil moisture observations.

(HEG tools version 2.8). This tool allows reprojection from the native MODIS Integerized Sinusoidal (ISIN) grid to the Universal Transverse Mercator (UTM) Zone 12 N projection used in our analysis. To minimize the effect of human-impacted regions, we created a mask excluding zones with minimal EVI changes over time (e.g., mines, urban areas and water bodies), thus focusing our analysis to areas of natural vegetation.

#### *Metrics of the spatial and temporal vegetation dynamics*

Remotely-sensed EVI data were characterized through: (1) temporal variations at each station; (2) derivation of vegetation metrics; (3) analysis of time stability of the spatiotemporal fields; and (4) identification of elevation controls on vegetation statistics. Temporal variations at specific sites were obtained by determining

the mean and standard deviation of EVI for each MODIS image from the  $3 \times 3$  pixels around a site. The arithmetic mean provides the averaged conditions at a site and accounts for uncertainties in the georeferencing of the station and the MODIS image. The standard deviation captures the spatial variability around an instrument site.

Temporal variations of EVI were used to estimate a set of vegetation metrics using the methods of Lloyd (1990) and Reed et al. (1994). With the original EVI time series, we generated two different moving averages: (1) a backward moving average (BMA) applied in reverse order and (2) a forward moving average (FMA). The moving averages were subsequently lagged by three time periods, each 16 days in length, to detect the crossing properties of the original EVI time series (e.g., timing of vegetation greening and senescence). We tested the sensitivity of the method to different

**Table 1**

Regional hydrometeorological station locations, altitudes and ecosystem classifications. The coordinate system for the locations is UTM 12 N, datum WGS84.

Station ID	Ecosystem	Easting (m)	Northing (m)	Altitude (m)
130	Sinaloan thornscrub	531,465	3,323,298	720
131	Sinaloan thornscrub	532,166	3,317,608	719
132	Sinaloan thornscrub	546,347	3,314,298	900
133	Sinaloan thornscrub	539,130	3,305,014	638
134	Madrean evergreen woodland	551,857	3,343,293	1180
135	Sonoran riparian deciduous woodland	546,349	3,346,966	1040
136	Sonoran desert scrub	532,579	3,353,405	1079
137	Sonoran savanna grassland	571,287	3,312,065	660
138	Sonoran savanna grassland	570,690	3,324,453	726
139	Sonoran savanna grassland	568,744	3,336,421	760
140	Sonoran savanna grassland	571,478	3,352,076	1013
143	Sonoran riparian deciduous woodland	542,590	3,356,533	960
144	Sonoran desert scrub	530,134	3,341,169	800
146	Madrean evergreen woodland	551,091	3,315,638	1385
147	Sinaloan thornscrub	544,811	3,290,182	620

lag lengths to best match the annual EVI cycle in the region (not shown).

Based on the above, we found the beginning of the vegetation greening as the crossing between the original EVI time series and the FMA. Similarly, the end of the greening season was found as the crossing between the EVI series and the BMA. Fig. 2a is an example of the original EVI data and their moving averages. Once the start and end of the greening are found, several vegetation metrics can be estimated (Reed et al., 1994): (1) Duration of Greenness (days), defined as the period between the onset and end of the

greenness; (2) Growing season integrated EVI (iEVI, dimensionless), measured as the area under the EVI series; (3) Seasonal range of EVI ( $\Delta\text{EVI}$ , dimensionless) determined from the maximum ( $\text{EVI}_{\text{max}}$ ) and minimum ( $\text{EVI}_{\text{min}}$ ) EVI values; and the (4) Days to  $\text{EVI}_{\text{max}}$ . Fig. 2b presents an example of the determination of the vegetation metrics for a Sinaloan thornscrub site during the 2004 growing season.

To analyze the temporal and spatial variability of EVI, we used the concepts of the spatial and temporal persistence (e.g., Vachaud et al., 1985; Jacobs et al., 2004; Vivoni et al., 2008a). We quantified the spatial and temporal root mean square error (RMSE) of the mean relative difference ( $\delta$ ) for each EVI pixel during the study period. The main difference between the spatial and temporal RMSE  $\delta$  is the mean used to compute the relative difference. For the spatial RMSE  $\delta_s$ , we used the spatial mean of each image and calculated the difference between every pixel and the spatial mean. Conversely, for the temporal RMSE  $\delta_t$ , we used the temporal mean for each pixel over all images and then calculated the difference between each pixel and its temporal mean.

To compute the spatial RMSE  $\delta_s$ , we first calculated the spatial mean of EVI in the region for each MODIS composite as:

$$\overline{\text{EVI}}_{sp,t} = \frac{1}{n} \sum_{s=1}^n \text{EVI}_{s,t}, \quad (1)$$

where  $\overline{\text{EVI}}_{sp,t}$  is the spatial mean EVI for each date ( $t$ ) over all pixels ( $s$ ) and  $n$  is the total number of pixels (i.e., 992,450 pixels,  $863 \times 1150$ ). Using this method, we obtained 83 spatially-averaged EVI values. Conversely, the temporal mean of EVI in each pixel is:

$$\overline{\text{EVI}}_{tm,s} = \frac{1}{N_t} \sum_{t=1}^{N_t} \text{EVI}_{s,t}, \quad (2)$$

where  $\overline{\text{EVI}}_{tm,s}$  is the temporal mean EVI and  $N_t$  is the total number of processed MODIS images (83 in total). In (1) and (2),  $\text{EVI}_{s,t}$  is the EVI value for pixel ( $s$ ) at time ( $t$ ). The mean relative difference captures the difference between a pixel and the mean (spatial or temporal) for all EVI images. The mean relative difference  $\bar{\delta}$  is computed as:

$$\bar{\delta} = \frac{1}{N_t} \sum_{t=1}^{N_t} \frac{\text{EVI}_{s,t} - \overline{\text{EVI}}}{\overline{\text{EVI}}}, \quad (3)$$

where  $\overline{\text{EVI}}$  is the spatial or temporal mean EVI, calculated by (1) or (2), respectively. The variance of the relative difference  $\sigma(\delta)^2$  is:

$$\sigma(\delta)^2 = \frac{1}{N_t - 1} \sum_{t=1}^{N_t} \left( \frac{\text{EVI}_{s,t} - \overline{\text{EVI}}}{\overline{\text{EVI}}} - \bar{\delta} \right)^2 \quad (4)$$

Finally, the root mean square error of the mean relative difference (RMSE  $\delta$ ) is a single metric which captures both the bias and the spread around the bias (Jacobs et al., 2004), computed as:

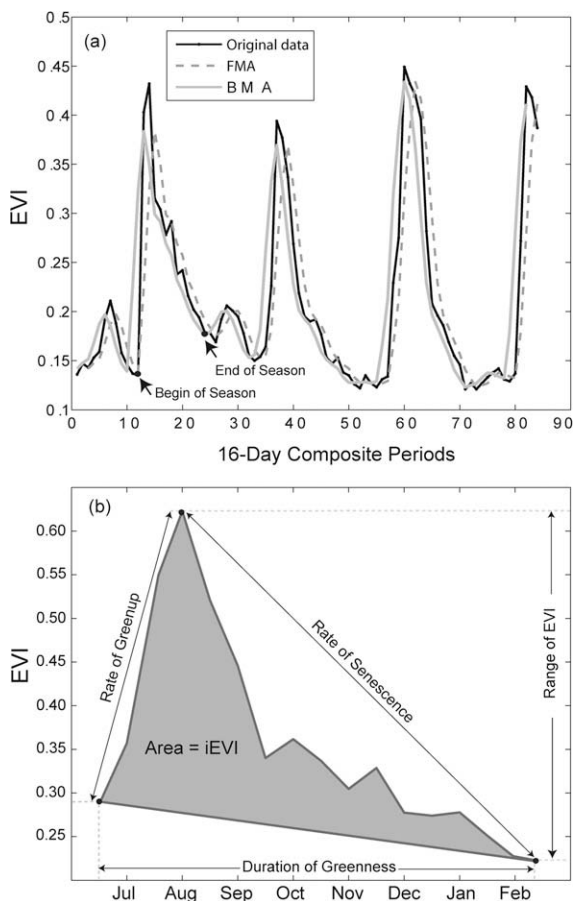


**Fig. 2.** Determination of vegetation metrics. (a) Identification of the beginning and end of the vegetation greening using EVI series and the backward (BMA) and forward (FMA) moving averages for station 130 (Sinaloan thornscrub). (b) Example of the vegetation metrics (iEVI,  $\Delta\text{EVI}$ , Rate of Greenup, Rate of Senescence and Duration of Greenness) for station 130 during the 2004 season.

$$RMSE \delta = (\bar{\delta}^2 + \sigma(\delta)^2)^{1/2} \quad (5)$$

Low RMSE  $\delta_s$  sites are stable pixels that closely track the spatially-averaged conditions in the region over time. This metric can identify ecosystems that capture the temporal EVI dynamics for an entire region. We would expect ecosystems that dominate the regional greening would exhibit low RMSE  $\delta_s$ . On the other hand, low RMSE  $\delta_t$  indicates pixels with values close to the temporal mean at the site and indicates ecosystems that have more limited seasonal changes. We expect that ecosystems with lower seasonality would exhibit low RMSE  $\delta_t$ .

We also established a topographic transect in the Río San Miguel to assess the variability of EVI and its statistical properties with elevation (Fig. 1). The transect is ~23 km in length, samples elevations from 600 to 1600 m, and traverses different ecosystems.

*Relationships between vegetation index (EVI), precipitation and soil moisture*

Several approaches were pursued to explore relations between EVI, precipitation and soil moisture. A linear regression between vegetation greening and precipitation was carried out using iEVI and accumulated seasonal rainfall. Due to sampling gaps, this analysis was focused on the 2005 monsoon. For this season, we also computed the greenness–precipitation ratio (GPR) to assess the efficiency of converting incoming rainfall into biomass. This ratio was computed as the iEVI divided by seasonal rainfall (mm) and multiplied by 100, to produce values close to unity. In addition, we calculated correlation coefficients between EVI and accumulated rainfall and time-averaged soil moisture using different monthly lags for 2005.

**Results and discussion**

*Spatial and temporal vegetation dynamics in regional ecosystems*

Fig. 3 presents spatial maps of the seasonal change in EVI ( $D_{EVI} = (EVI_{max} - EVI_{min})/EVI_{min}$ , expressed as a percentage) for the three monsoons. Clearly, there are variations in the  $D_{EVI}$  pattern re-

lated to ecosystem distributions, terrain characteristics and rainfall amounts. The distribution and range of  $D_{EVI}$  vary for each year, following the total rainfall averaged over all stations ( $\bar{R}_s$ ) from July to September. In 2004 ( $\bar{R}_s = 251$  mm), the largest amount of vegetation greening occurred in the southeastern part of the domain. The area between stations 146 and 147 in the Río San Miguel also exhibited high greening, in agreement with the elevated soil moisture observed by Vivoni et al. (2008a). In contrast, 2005 was the driest year in the study ( $\bar{R}_s = 222$  mm) and experienced the smallest  $D_{EVI}$ , ranging from 50% to 150%. Note, however, that isolated patches had high degrees of greening, suggesting localized storms during this monsoon. Conversely, the year 2006 had the largest change in EVI due to the elevated precipitation ( $\bar{R}_s = 350$  mm) and the preceding dry winter. Note that  $D_{EVI}$  is also more uniform, indicating that the ecosystem responses were vigorous and spatially extensive. Interestingly, smaller changes in seasonal EVI are observed in riparian areas (Sonoran riparian deciduous woodland) and high mountains (Madrean montane conifer forests) as these remain green throughout the year. Overall, the spatial EVI fields clearly show that the seasonal and interannual changes in vegetation are linked to rainfall, ecosystem pattern and topography.

Fig. 4 presents the temporal variations of EVI, precipitation and soil moisture from January 2004 to June 2007 (16-day intervals) at: (a) station 146 (Madrean evergreen woodland), (b) station 132 (Sinaloan thornscrub), (c) station 139 (Sonoran savanna grassland), and (d) station 144 (Sonora desert scrub). Temporal variations in EVI are dramatic in each ecosystem and related to the hydrologic conditions at each site. The Madrean evergreen woodland (Fig. 4a) exhibited the highest precipitation in the region, with an exceptional rainfall in 2006 (>300 mm in July). In response, soil moisture was elevated in 2006, reaching >20% in the surface soil layer. This plant-available water led to a vigorous summer greening reflected in a peak EVI of 0.55. In contrast, Sinaloan thornscrub (Fig. 4b) showed less rainfall than higher sites, but more consistent greening across the summers, suggesting this ecosystem is fairly resilient to hydrologic changes. Sonoran savanna grasslands (Fig. 4c) have a more muted response (smaller EVI range, with the exception of year 2005) as compared to the other ecosystems. Nevertheless, the EVI exhibits high temporal variations in response to wet and dry periods, including a spring peak in 2005 after a wet

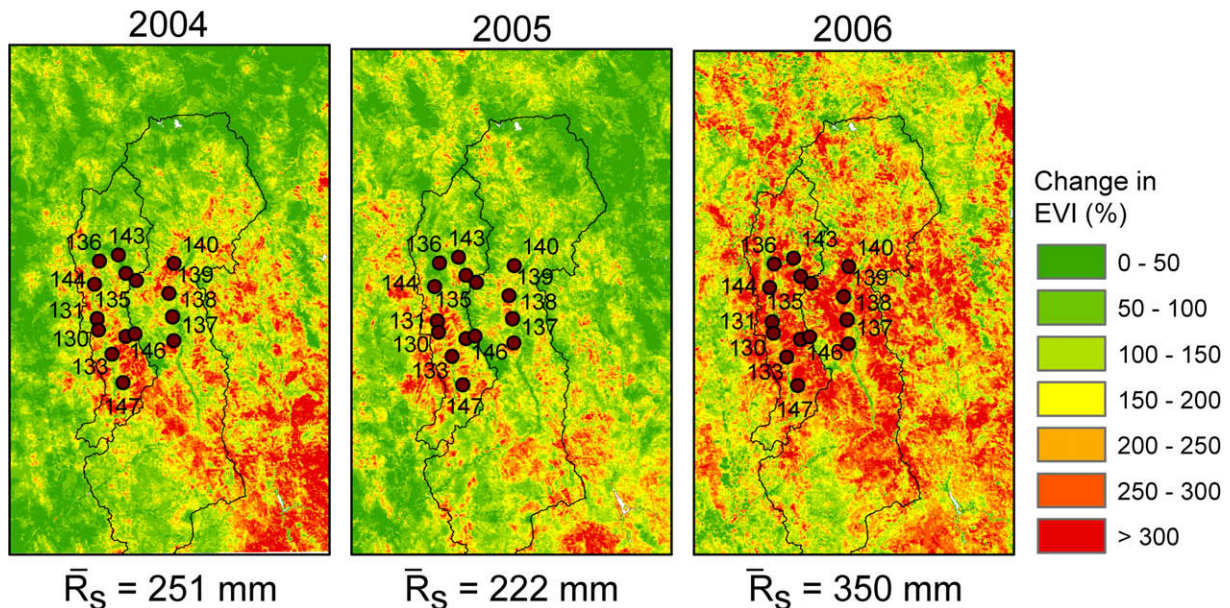


**Fig. 3.** Comparison of seasonal EVI change (%). The percentage of EVI change is calculated using the lowest and highest EVI for a particular summer season (2004–2006).  $\bar{R}_s$  is the total summer rainfall (July–September) averaged over all stations.

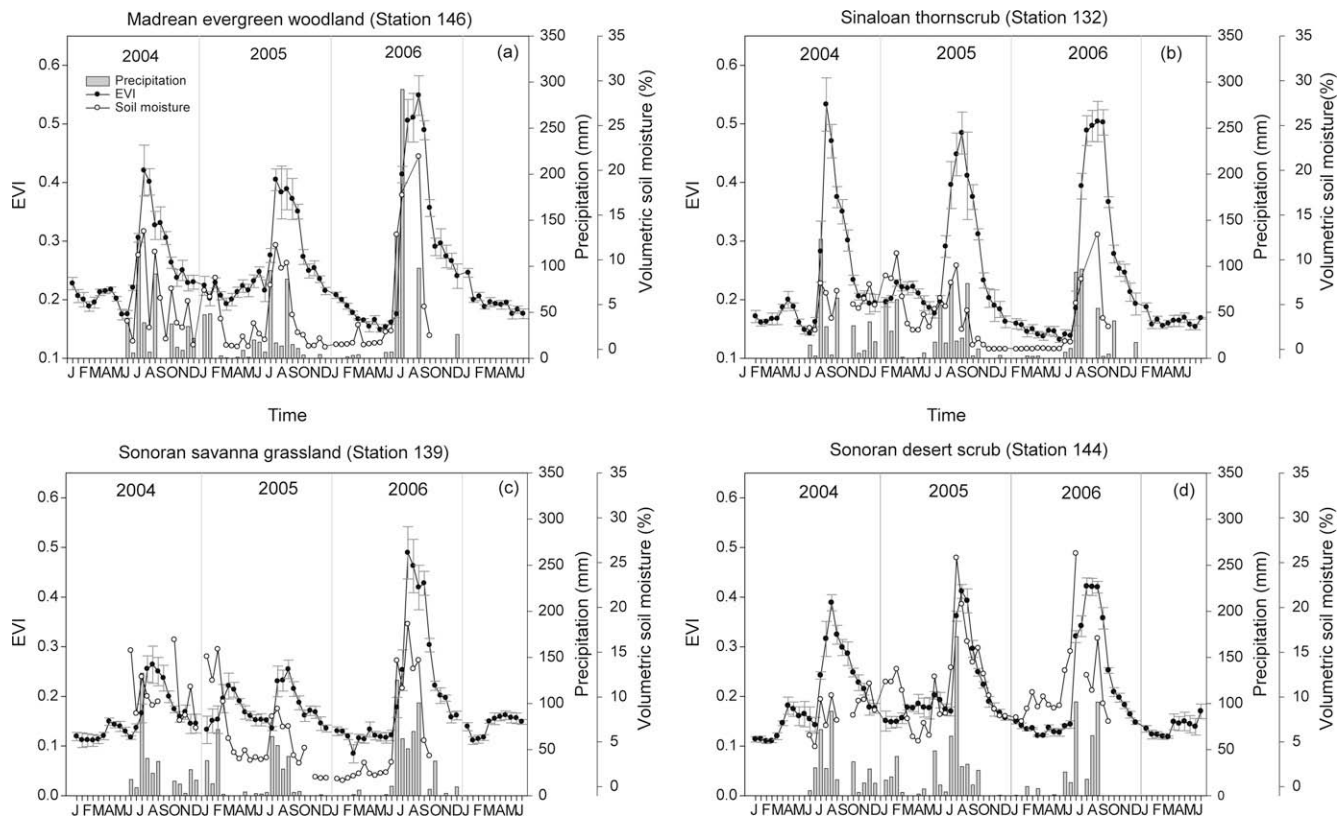


**Fig. 4.** Temporal variation of EVI among different regional ecosystems: (a) Madrean evergreen woodland (station 146), (b) Sinaloan thornscrub (station 132), (c) Sonoran savanna grassland (station 139), and (d) Sonoran desert scrub (station 144). EVI symbols correspond to the average value calculated in the  $3 \times 3$  pixel region around each station for each composite. The vertical bars depict the  $\pm 1$  standard deviation of the  $3 \times 3$  pixel region. Precipitation (mm) is accumulated during 16-day intervals (gray bars), while the surface soil moisture (%) is averaged during the 16-day periods (open circles).

winter. Finally, the Sonoran desert scrub (Fig. 4d) also experiences summer greening, with small interannual variations. Interestingly, summer 2005 had more favorable hydrologic conditions than 2006 at this station and thus the highest peak EVI in the three-year record.

#### Quantifying ecosystem dynamics through vegetation metrics

Vegetation metrics can quantify ecosystem responses to precipitation and surface soil moisture during the NAM. Table 2 presents the phenological metrics obtained for each station from 2004 to 2006. Overall, the vegetation metrics, in particular the iEVI and  $\Delta$ EVI, confirm that 2006 had the most dramatic greening in most of the stations. In contrast, some stations during 2004 had low Duration of Greenness and Days to EVI<sub>max</sub> as well as the smallest iEVI and  $\Delta$ EVI. However, other stations showed lower vegetation metrics in 2005. This indicates that regional rainfall was not homogeneous and some stations receive more rainfall than others in different years.

The metrics also reveal differences and similarities in vegetation productivity among the stations. Stations with common plant communities share similar response to summer rainfall. For example, lower productivity stations are all in Sonoran savanna grasslands (stations 137, 138 and 139) with low iEVI,  $\Delta$ EVI and Duration of Greenness. Similarities are also observed in vegetation metrics for the Sonoran riparian deciduous woodland sites (stations 135 and 143). For the wet 2006 summer, however, precipitation amount and soil water availability lead to certain degrees of homogenization in the vegetation response across all ecosystems. For instance, Madrean evergreen woodlands (station 146) and Sinaloan thornscrub (station 132) share similar responses in

2006 (iEVI = 4.79 and 4.65 for 2006), despite having different plant communities. Differences in vegetation metrics among stations are stronger during drier monsoons. It is interesting to note that the Madrean evergreen woodland and Sinaloan thornscrub appear to have different strategies to cope with interannual hydrologic changes. Evergreen woodlands vary their maximum greening (EVI<sub>max</sub>) in response to increased rainfall amounts, while deciduous trees and shrubs vary the growing season productivity (iEVI). These two plant greenup strategies may explain how these ecosystems exist at different elevations in the region.

To explore this further, Table 3 presents temporal coefficients of variation (CVs) for each vegetation metric computed for the average conditions in each ecosystem across all years. As a result, the CV primarily captures the interannual variations in vegetation metrics in a particular ecosystem. Ecosystems with high CVs imply large interannual changes. Sonoran savanna grassland have higher CVs for iEVI,  $\Delta$ EVI, indicating strong variations between years. Small CV in iEVI and high CV in  $\Delta$ EVI are observed in the Sonoran desert scrub, suggesting this ecosystem varies primarily in the EVI range from year-to-year. Finally, the vegetation metric with the highest interannual variation is Days to EVI<sub>max</sub>, indicating that the rate of ecosystem greening is highly influenced by rainfall amounts during the monsoon onset.

#### Spatial and temporal stability analyses of vegetation dynamics

The ecosystem response to precipitation and soil moisture conditions can be discerned through spatial and temporal persistence of the EVI fields. Regions with low spatial RMSE  $\delta_s$  (Fig. 5a, red colors) correspond to zones that closely track the spatially-averaged conditions. These areas coincide well with the location of Sinaloan

**Table 2**  
Comparison of vegetation metrics for the regional stations during the three monsoon periods.

Station ID	Ecosystem	Year	iEVI (-)	EVI <sub>max</sub> (-)	EVI <sub>min</sub> (-)	ΔEVI (-)	Greening duration (days)	Days to EVI <sub>max</sub> (days)
130	Sinaloan thornscrub	2004	3.45	0.43	0.14	0.30	208	32
		2005	3.61	0.39	0.13	0.27	272	48
		2006	3.80	0.45	0.12	0.33	240	64
131	Sinaloan thornscrub	2004	3.37	0.42	0.13	0.28	192	48
		2005	3.20	0.47	0.13	0.34	208	64
		2006	3.82	0.46	0.12	0.34	256	80
132	Sinaloan thornscrub	2004	3.28	0.53	0.14	0.39	176	48
		2005	4.65	0.48	0.14	0.34	288	80
		2006	4.45	0.50	0.14	0.37	224	80
133	Sinaloan thornscrub	2004	3.08	0.38	0.15	0.23	192	48
		2005	3.28	0.49	0.15	0.33	208	64
		2006	3.97	0.43	0.13	0.30	208	64
134	Madrean evergreen woodland	2004	3.53	0.32	0.11	0.21	304	144
		2005	3.90	0.28	0.12	0.17	352	176
		2006	2.99	0.34	0.12	0.23	224	64
135	Sonoran riparian woodland	2004	2.76	0.32	0.14	0.18	192	48
		2005	3.13	0.44	0.13	0.31	208	32
		2006	3.86	0.49	0.11	0.38	256	80
136	Sonoran desert scrub	2004	3.48	0.41	0.13	0.28	208	32
		2005	3.14	0.43	0.13	0.31	224	48
		2006	3.65	0.48	0.13	0.36	224	48
137	Sonoran savanna grassland	2004	1.81	0.35	0.12	0.24	128	48
		2005	2.44	0.36	0.14	0.22	176	32
		2006	3.78	0.44	0.13	0.32	224	48
138	Semi-desert grassland	2004	2.30	0.26	0.14	0.12	192	48
		2005	2.95	0.37	0.13	0.24	240	32
		2006	3.95	0.49	0.10	0.39	224	64
139	Sonoran savanna grassland	2004	2.28	0.26	0.12	0.15	192	64
		2005	2.28	0.25	0.12	0.14	208	48
		2006	3.72	0.49	0.11	0.38	224	48
140	Semi-desert grassland	2004	2.81	0.37	0.12	0.26	192	32
		2005	2.63	0.32	0.11	0.21	240	32
		2006	3.59	0.48	0.11	0.37	224	48
143	Sonoran riparian woodland	2004	2.41	0.37	0.14	0.23	160	32
		2005	2.97	0.38	0.13	0.25	208	32
		2006	3.80	0.51	0.10	0.41	240	96
144	Sonoran desert scrub	2004	3.05	0.39	0.14	0.25	192	48
		2005	3.32	0.41	0.12	0.29	240	32
		2006	4.10	0.42	0.12	0.30	272	80
146	Madrean evergreen woodland	2004	3.72	0.42	0.18	0.25	208	48
		2005	4.69	0.41	0.15	0.25	288	32
		2006	4.79	0.55	0.16	0.39	224	80
147	Sinaloan thornscrub	2004	1.91	0.35	0.12	0.23	112	32
		2005	2.80	0.41	0.12	0.29	224	48
		2006	3.82	0.45	0.11	0.34	224	48

thornscrub and Sonoran desert scrub (Brown, 1994) that exhibit strong seasonal variations in EVI and occupy large regional extents. Note these areas are located over a range of elevations, but are not observed in the highest peaks and riparian corridors. In these locations, high spatial RMSE  $\delta_s$  (Fig. 5a, blue colors) indicate ecosystems behaving differently from the spatial mean and correspond to Madrean evergreen woodland and conifer forests at high elevations and Sonoran riparian deciduous woodland along rivers. Clearly, the distribution of RMSE  $\delta_s$  is useful for distinguishing between evergreen woodlands at high elevations and deciduous scrublands at mid-elevations.

The temporal RMSE  $\delta_t$  (Fig. 5b) supports the above analysis by distinguishing locations that closely track the temporal mean in each pixel. Regions with low RMSE  $\delta_t$  (blue colors) have relatively smaller changes in time and correspond to Madrean evergreen woodland and conifer forests at high elevations and Sonoran riparian deciduous woodlands. Despite having deciduous trees, the riparian woodlands can directly access groundwater and remain

**Table 3**

Coefficient of variation (CV) of vegetation metrics for different ecosystems during the period 2004–2006. CV is calculated as the temporal standard deviation divided by the temporal mean over all stations in each ecosystem ( $N$  sites per ecosystem).

Ecosystem	$N$	Coefficient of variation (CV)		
		iEVI	ΔEVI	Days to EVI <sub>max</sub>
Madrean evergreen woodland	2	0.24	0.25	0.70
Sinaloan thornscrub	5	0.19	0.15	0.28
Sonoran savanna grassland	4	0.25	0.38	0.25
Sonoran desert scrub	2	0.11	0.27	0.48
Sonoran riparian deciduous forest	2	0.18	0.34	0.55

green during longer time periods. Lower temporal persistence is observed for regions with high RMSE  $\delta_t$  (red colors) which depict zones with large temporal changes. Clearly, these match the areas with low RMSE  $\delta_s$ , in particular the Sinaloan thornscrub and Sonoran desert scrub. The temporal RMSE  $\delta_t$  is able to more clearly

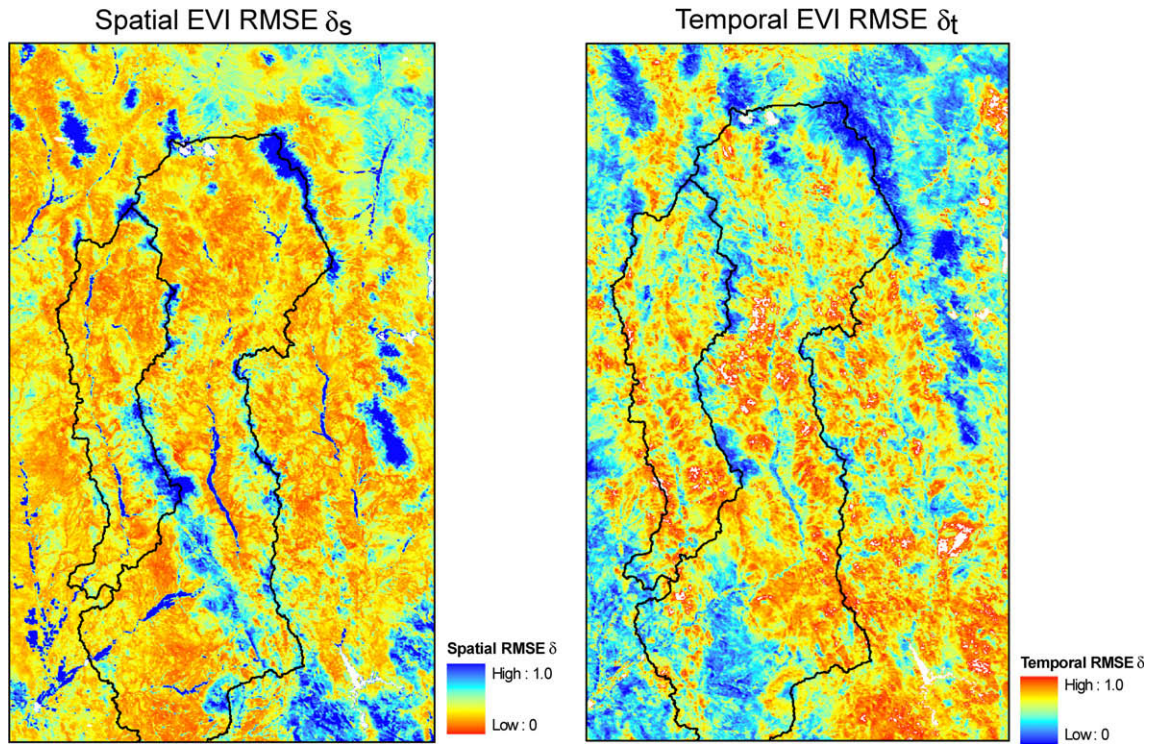


Fig. 5. Temporal and spatial RMSE of the mean relative difference ( $\delta$ ) in the Río San Miguel and Río Sonora basins.

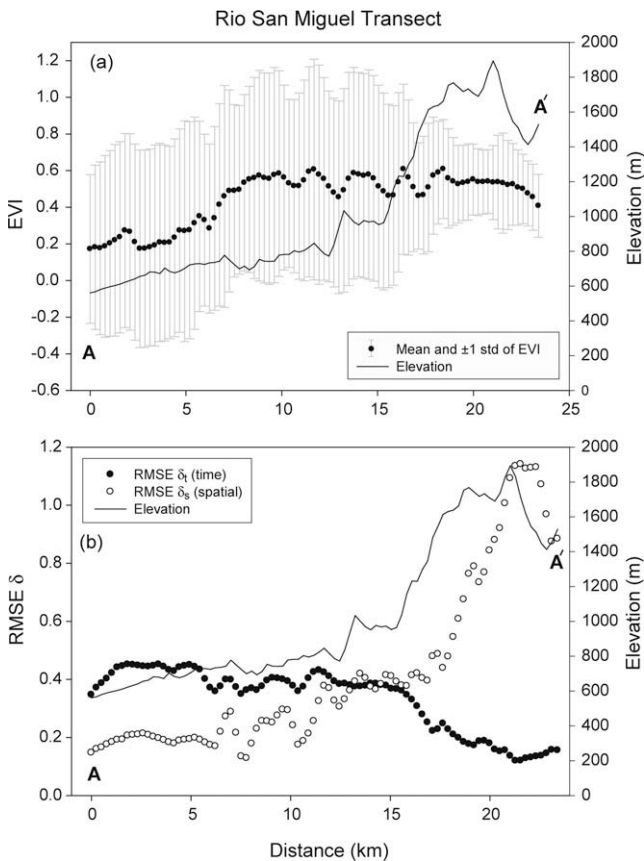


Fig. 6. (a) Relation between elevation and temporal mean (closed circles) and temporal standard deviation of EVI ( $\pm 1$  std as vertical bars). (b) Relation between elevation and the spatial and temporal RMSE  $\delta$ .

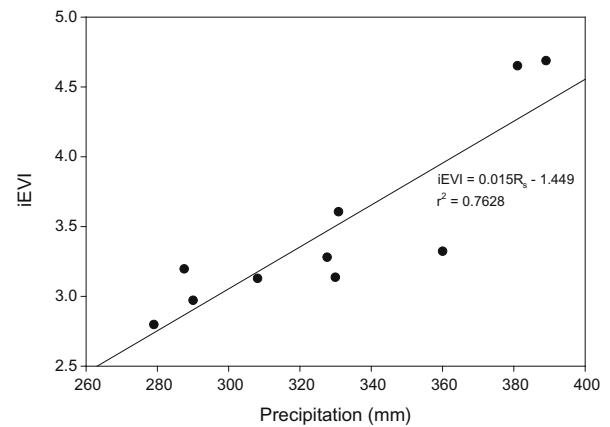
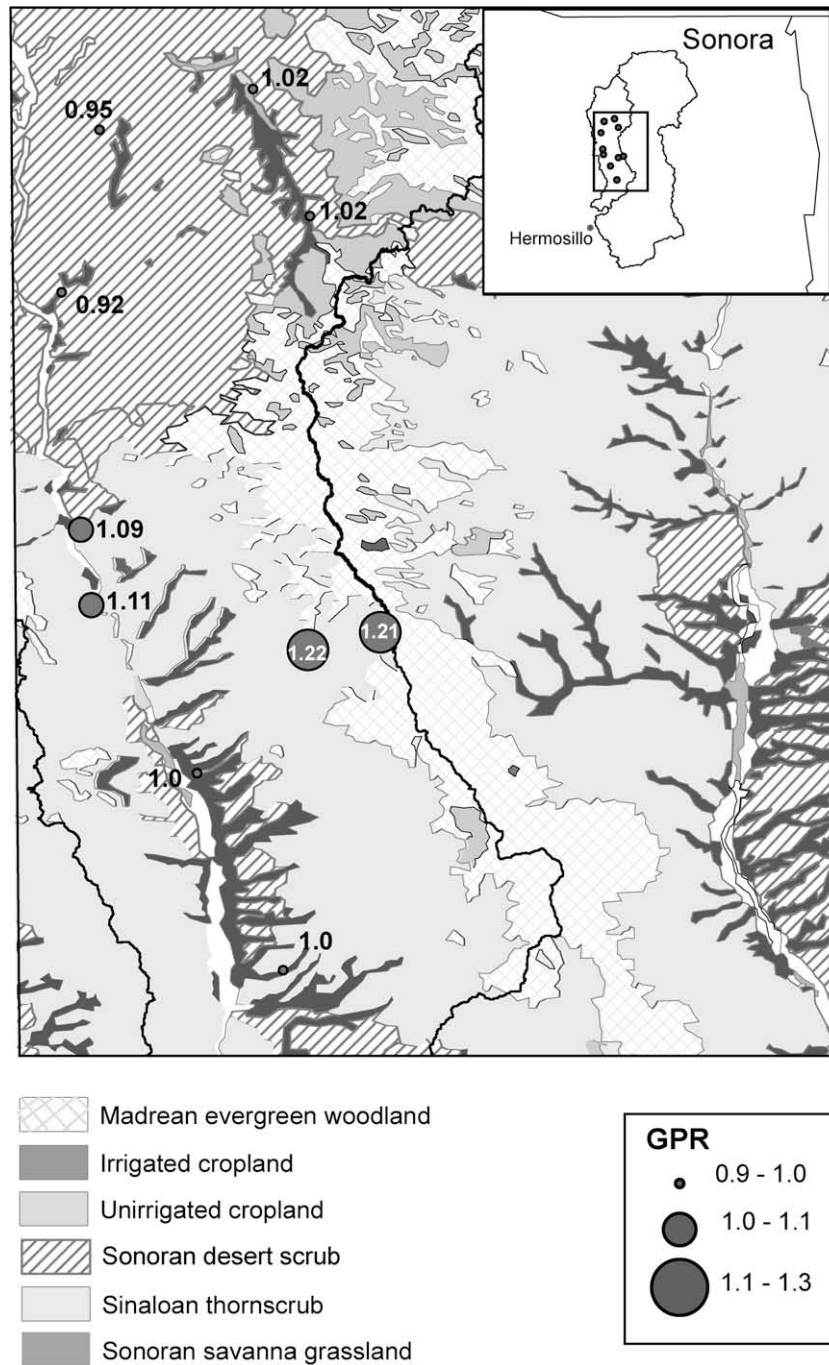


Fig. 7. Relation between iEVI and seasonal precipitation accumulation for the monsoon season in 2005.

separate these two ecosystems, with Sinaloan thornscrub further south in the domain and replaced by Sonoran desert scrub at similar altitudes in the north. In conjunction, the spatial and temporal persistence maps reveal ecosystem patterns that are not observed through simpler metrics such as seasonal EVI changes (Fig. 3). Further, this analysis extends applications of RMSE  $\delta$  beyond soil moisture studies (e.g., Jacobs et al., 2004; Vivoni et al., 2008a).

To explore elevation controls, Fig. 6 presents the variation of EVI, RMSE  $\delta_s$  and RMSE  $\delta_t$  for a topographic transect in Río San Miguel (see A–A' in Fig. 1). The transect was selected to capture a range of elevations (550–1900 m) and span several ecosystems. The temporal mean EVI (symbols) increases with elevation, while the temporal standard deviation (vertical bars depict  $\pm 1$  std) typically decreases with altitude. These variations indicate that the mid-elevation Sinaloan thornscrub and Sonoran desert scrub are characterized by lower time-averaged greenness, which is more



**Fig. 8.** Distribution of greenness–precipitation ratio (GPR in  $\text{mm}^{-1} \times 100$ ) at the regional stations (note that the region of interest is indicated in the inset by the square polygon). For reference, the spatial distribution of ecosystems as mapped by INEGI (Instituto Nacional de Estadística, Geografía e Informática) is shown.

variable in time, as compared to the high elevation Madrean evergreen woodland. The mid-elevation ecosystems exhibit low spatial RMSE  $\delta_s$  and high temporal RMSE  $\delta_t$ , which indicate areas closely tracking the mean conditions in the region. These elevations correspond to Sinaloan thornscrub and Sonoran desert scrub which are highly responsive to NAM precipitation and occupy large regional extents. At high elevations, the Madrean evergreen woodland has a larger spatial RMSE  $\delta_s$  and a smaller temporal RMSE  $\delta_t$ . This suggests that the evergreen species have time-stable conditions that do not track the spatially-averaged response. A range of elevations (~600–900 m) simultaneously have small spatial and temporal RMSE  $\delta$ . We interpret this as an elevation band of significant monsoonal response that dominates the regional greening, as sug-

gested by Vivoni et al. (2007). Clearly, spatial and temporal persistence reveal variations in vegetation dynamics along topographic transects and can aid in the interpretation of vegetation–elevation relations in semiarid mountain fronts.

#### Relations between vegetation and hydrologic indices

To explore the relation between vegetation dynamics and hydrologic conditions, we compared iEVI, the greenness–precipitation ratio ( $\text{GPR} = (\text{iEVI}/R_s) \times 100$ ) and the total precipitation ( $R_s$ ) at each station for the 2005 monsoon. This particular summer was selected due to its limited amounts of missing data, resulting in the decrease of the number of analyzed stations from 15 to 10. Fig. 7

presents the linear relation between iEVI and precipitation ( $R_s$ ). Clearly, as rainfall amounts increase across the regional stations, ecosystem productivity during the summer monsoon increases. While ecophysiological differences are present in the regional ecosystems, seasonal rainfall is a good predictor of biomass production (iEVI). Results are consistent with other studies, where higher vegetation productivity was observed with increasing rainfall (e.g., Li et al., 2004; Prasad et al., 2005). Further testing of the proposed relation during other summers and for a larger number of stations may provide an indication of its robustness.

The GPR for summer 2005 is presented in Fig. 8 as a map overlaid on the regional ecosystems. As shown in Table 4, the range in GPR among the stations is from 0.92 (station 144, Sonoran desert scrub) to 1.22 (station 132, Sinaloan thornscrub). The spatial variability in GPR indicates that ecosystems in the southern region of the Río San Miguel more efficiently use precipitation for biomass production. Interestingly, each of these ecosystems corresponds to the Sinaloan thornscrub (stations 130, 131, 132, 133, 147), suggesting that this plant community is well-tuned to utilizing summer rainfall to produce vegetation greening. The response in the Sinaloan thornscrub is consistent with seasonal changes in EVI for 2005 (Fig. 3b) and a high temporal RMSE  $\delta_t$  (Fig. 5b). Other regional ecosystems, such as Sonoran savanna grassland (stations 137, 138, 139) and Sonoran riparian deciduous woodland (stations 135, 143), show smaller GPR, suggesting lower rainfall use efficiency in grasslands and riparian trees. Lower GPR in riparian sites, despite access to groundwater, is likely due to human impacts in

the areas leading to decreased groundwater levels and to land cover changes associated with agriculture.

The relation between vegetation dynamics and surface soil moisture in each station are explored using lagged Pearson correlation coefficients (CCs) for 2005. Results are shown as average values (symbols) over all stations and their variability as the  $\pm 1$  standard deviation (vertical bars). Fig. 9 reveals that most stations have strong correlations between EVI and accumulated rainfall in the prior months, while the CCs are somewhat lower in the current month (lag 0). This suggests that the regional ecosystem responses depend on the accumulated seasonal rainfall, with limited controls of the current rainfall conditions alone. Conversely, the correlation coefficients between monthly EVI and time-averaged soil moisture exhibit larger values for the current (lag 0) and current and previous (lag 0 + 1) months. The higher CCs observed at the shorter monthly lags between EVI and surface soil moisture confirms that the latter controls the vegetation dynamics. This is clear evidence that concurrent surface soil moisture (5-cm depth) is central in converting precipitation into plant-available water used for vegetation greening.

## Summary and conclusions

Vegetation dynamics in the NAM region are linked to seasonal changes in precipitation (e.g., Salinas-Zavala et al., 2002; Matsui et al., 2005; Watts et al., 2007; Vivoni et al., 2007). To the authors' knowledge, however, the controls exerted by soil moisture on seasonal vegetation greening have not been studied for the broader NAM region. Furthermore, the seasonal, interannual and spatial variations in vegetation response during the NAM are not well understood. Quantifying these spatiotemporal variations in a range of ecosystems is fundamental for assessing the degree of coupling between ecologic, hydrologic and atmospheric processes during the summer season. In this study, we quantify the seasonal and interannual changes in vegetation greenness through the use of remotely-sensed EVI fields from MODIS during 2004–2006. Our regional analysis focuses on a large area in northern Sonora comprised by two major basins. The regional extent and the study duration were selected to take advantage of an instrument network with precipitation and soil moisture observations. By relating the remotely-sensed and ground data sets, we identify the following characteristics of the regional vegetation dynamics and their relation to precipitation and soil moisture:

- (1) Seasonal changes in vegetation greenness are dramatic in all the regional ecosystems and are related to hydrologic conditions and their spatial distribution during a particular monsoon season. As a result, interannual variability is observed in the seasonal vegetation greening and the metrics used to quantify biomass production. The vegetation response was most intense and extensive during the wet 2006 monsoon, reaching up to a 300% seasonal increase in EVI.
- (2) Vegetation responses to NAM precipitation and soil moisture depend strongly on the plant communities in each ecosystem. The ecosystem with consistently high monsoon greening is the mid-elevation Sinaloan thornscrub, as suggested by Watts et al. (2007) and Vivoni et al. (2007). Other ecosystems in the region either exhibited lower seasonal changes in EVI or less consistent year-to-year variations. Comparisons across ecosystems indicate that different plant greening strategies are utilized in response to interannual hydrologic variations.
- (3) Spatial and temporal persistence of remotely-sensed EVI fields reveal ecosystem patterns that are not observed using simple metrics. In particular, RMSE  $\delta_s$  distinguishes between

**Table 4**

Comparison of iEVI, precipitation (mm) and greenness–precipitation ratio (GPR in  $\text{mm}^{-1} \times 100$ ) for the available regional stations during 2005. Greenness–precipitation ratio is computed as a function of the iEVI divided by seasonal rainfall (mm) and multiplied by 100.

Station ID	iEVI (–)	Precipitation (mm)	GPR ( $\text{mm}^{-1}$ ) $\times 100$
130	3.61	330.80	1.09
131	3.20	287.50	1.11
132	4.65	381.00	1.22
133	3.28	327.60	1.00
135	3.13	308.10	1.02
136	3.14	329.90	0.95
143	2.97	290.00	1.02
144	3.32	360.00	0.92
146	4.69	389.00	1.21
147	2.80	279.00	1.00

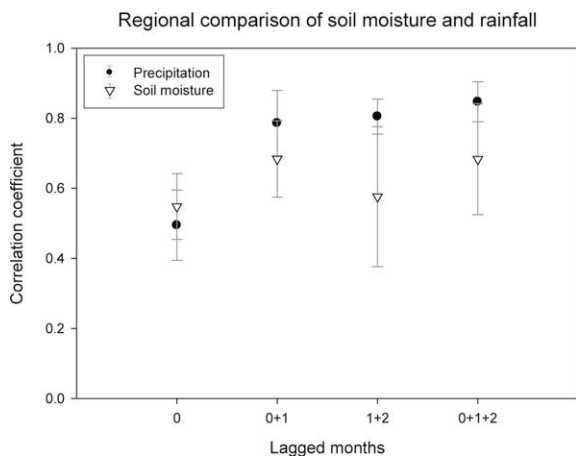


**Fig. 9.** Linear correlation coefficients (CCs) between monthly EVI and accumulated precipitation and averaged soil moisture over a range of different monthly lags, arranged from current (lag 0) toward longer prior periods (lag 0 + 1 + 2). CCs are shown as averages (symbols) and standard deviations ( $\pm 1$  std as vertical bars) over all stations in 2005.

evergreen woodlands at high elevations and deciduous scrublands at mid-elevations, while the temporal RMSE  $\delta_t$  can more clearly separate different ecosystems at similar elevations. Analysis along a topographic transects indicate that elevation controls vegetation dynamics and serves to organize ecosystems into elevation bands, with high monsoonal response at mid-elevations.

- (4) Accumulated seasonal precipitation is a strong indicator of greenness intensity across the regional ecosystems, with Sinaloa thornscrub exhibiting the highest greenness–precipitation ratio (GPR). During the study period, differences between ecosystem responses were minimized during the wet 2006 monsoon and maximized during drier monsoons, in contrast to the common rainfall use efficiency found by Huxman et al. (2004) during drought. Additional studies are required to quantify greenness–precipitation ratio in wet and dry periods in the region.
- (5) Lagged correlation analysis indicates a strong degree of coupling between vegetation greening and hydrologic conditions at each regional station. Concurrent correlations for monthly EVI with surface soil moisture and precipitation are comparable, while lagged correlations are more significant for the accumulated precipitation. This suggests that soil moisture plays an important and immediate role in vegetation response inside the NAM region.

The observational analysis and interpretations conducted here show the importance of combining satellite remote sensing and ground networks for monitoring ecosystem dynamics and their link to precipitation and surface soil moisture conditions. Clearly, the study duration is a limitation in our interannual analysis, primarily due to the recent establishment of the regional network. Nevertheless, significant interannual variability in vegetation dynamics were observed in the three monsoon seasons, including one of the driest (2005) and wettest (2006) seasons in the period 1985–2006 (e.g., Dominguez et al., 2008). Additional analysis is desirable either by extending the work as new datasets become available or by performing retrospective analysis with satellite data (though ground data would be limited) over the current basins or the broader NAM region. In particular, expanding this analysis to include relations with root zone soil moisture observations (top 1-m, where available) would be desirable. Another focus should be on identifying the long-term interannual vegetation variability and its relation to precipitation, which itself exhibits year-to-year changes due to several factors, including sea surface temperature (Castro et al., 2007) and continental snow and soil moisture anomalies (Gutzler, 2000; Zhu et al., 2007). If the link between interannual precipitation variations and vegetation response can be identified, enhanced predictability of the land surface response to the North American monsoon would be possible.

## Acknowledgements

We acknowledge funding from the National Science Foundation IRES program (Grant OISE 0809946), the NOAA Climate Program Office (Grant CPPA GC07-019), the US Fulbright Program to E.R.V and the Consejo Nacional de Ciencias y Tecnología (CONACYT) fellowship to the first author. We also thank two reviewers whose suggestions helped to improve earlier versions of the manuscript.

## References

- Bindlish, R., Jackson, T.J., Gasiewski, A.J., Stankov, B., Cosh, M.H., Mladenova, I., Vivoni, E.R., Lakshmi, V., Watts, C.J., Keefer, T., 2008. Aircraft-based soil moisture retrievals in mixed vegetation and topographic conditions. *Remote Sensing of Environment* 112 (2), 375–390.
- Bounoua, L., Collatz, C.J., Los, S.O., Sellers, P.J., Dazlich, D.A., Tucker, C.J., Randall, D.A., 2000. Sensitivity of climate to NDVI changes. *Journal of Climate* 13, 2277–2292.
- Breshears, D.D., Barnes, F.J., 1999. Interrelationships between plant functional types and soil moisture heterogeneity for semiarid landscapes within the grassland/forest continuum: a unified conceptual model. *Landscape Ecology* 14 (5), 465–478.
- Brown, E.D., 1994. *Biotic Communities: Southwestern United States and Northwestern Mexico*. University of Utah Press, 342 pp.
- Calvet, C., Noilhan, J., Bessemoulin, P., 1998. Retrieving the root-zone soil moisture from surface soil moisture or temperature estimates: a feasibility study based on field measurements. *Journal of Applied Meteorology* 37, 371–386.
- Caso, M., Gonzalez-Abraham, C., Ezcurra, E., 2007. Divergent ecological effects of oceanographic anomalies on terrestrial ecosystems of the Mexican Pacific coast. *Proceedings of the National Academy of Sciences* 104 (25), 10530–10535.
- Casper, B.B., Schenk, H.J., Jackson, R.B., 2003. Defining plant's belowground zone of influence. *Ecology* 84, 2313–2321.
- Castro, C.L., Pielke, R.A., Adegoke, J.O., Schubert, S.D., Pegion, P.J., 2007. Investigation of the summer climate of the contiguous United States and Mexico using the regional atmospheric modeling system (RAMS). Part II: model climate variability. *Journal of Climate* 20 (15), 3866–3887.
- Chamaille-Jammes, S., Fritz, H., Murindagomo, F., 2006. Spatial patterns of the NDVI–rainfall relationship at the seasonal and inter-annual time scales in an African savanna. *International Journal of Remote Sensing* 27 (23), 5185–5200.
- Chen, M., Xie, P., Janowiak, J.E., Arkin, P.A., 2002. Global land precipitation: a 50-yr monthly analysis based on gauge observations. *Journal of Hydrometeorology* 3, 249–266.
- Coblentz, D.D., Riitters, K.H., 2004. Topographic controls on the regional-scale biodiversity of the south-western USA. *Journal of Biogeography* 31 (7), 1125–1138.
- Davenport, M.L., Nicholson, S.E., 1993. On the relationship between rainfall and the Normalized Difference Vegetation Index for diverse vegetation types in East Africa. *International Journal of Remote Sensing* 14 (12), 2369–2389.
- De Lannoy, J.M., Verhoest, N.C., Houser, P.R., Gish, T.J., Van Meirvenne, M., 2006. Spatial and temporal characteristics of soil moisture in an intensively monitored agricultural field (OPE3). *Journal of Hydrology* 331 (3–4), 719–730.
- Dominguez, F., Kumar, P., Vivoni, E.R., 2008. Precipitation recycling variability and ecoclimatological stability – a study using NARR data. Part II: North American Monsoon Region. *Journal of Climate* 21, 5187–5203.
- Douglas, M.W., Maddox, R.A., Howard, K., Reyes, S., 1993. The Mexican monsoon. *Journal of Climate* 6 (8), 1665–1677.
- Famiglietti, J.S., Rudnicki, W., Rodell, M., 1998. Variability in surface moisture content along a hillslope transect: Rattlesnake Hill, Texas. *Journal of Hydrology* 210 (1–4), 259–281.
- Gochis, D.J., Watts, C.J., Garatuza-Payan, J., Rodríguez, J.C., 2007. Spatial and temporal patterns of precipitation intensity as observed by the NAME Event Rain gauge Network from 2002 to 2004. *Journal of Climate* 20 (9), 1734–1750.
- Goward, N.S., 1989. Satellite bioclimatology. *Journal of Climate* 2 (7), 710–720.
- Guillevic, P., Koster, R.D., Suarez, M.J., Bounoua, L., Collatz, C.J., Los, S.O., Mahanama, S.P.P., 2002. Influence of the interannual variability of vegetation on the surface energy balance: a global sensitivity study. *Journal of Hydrometeorology* 3 (6), 617–629.
- Gutzler, D.S., 2000. Covariability of spring snowpack and summer rainfall across the southwest United States. *Journal of Climate* 13 (22), 4018–4027.
- Higgins, R.W., Gochis, D.J., 2007. Synthesis of results from the North American Monsoon Experiment (NAME) process study. *Journal of Climate* 20 (9), 1601–1607.
- Huete, A.R., Liu, H.Q., Batchily, K., vanLeeuwen, W., 1997. A comparison of vegetation indices global set of TM images for EOS-MODIS. *Remote Sensing of Environment* 59 (3), 440–451.
- Huete, A.R., Didan, K., Miura, T., Rodriguez, E.P., Gao, X., Ferreira, L.G., 2002. Overview of the radiometric and biophysical performance of the MODIS vegetation indices. *Remote Sensing of Environment* 83 (1–2), 195–213.
- Huxman, T.E., Smith, M.D., Fay, P.A., Knapp, A.K., Shaw, M.R., Loik, M.E., Smith, S.D., Tissue, D.T., Zak, J.C., Weltzin, J.F., Pockman, W.T., Sala, O.E., Haddad, B.M., Harte, J., Koch, G.W., Schwinning, S., Small, E.E., Williams, D.G., 2004. Convergence across biomes to a common rain-use efficiency. *Nature* 429, 651–654.
- Jacobs, M.J., Mohanty, P.B., Hsu, C.E., Miller, D., 2004. SMEX02: field scale variability, time stability and similarity of soil moisture. *Remote Sensing of Environment* 92 (4), 436–446.
- Li, D., Lewis, J., Rowland, J., Tappan, G., Tieszen, L.L., 2004. Evaluation of land performance in Senegal using multi-temporal NDVI and rainfall series. *Journal of Arid Environments* 59 (3), 463–480.
- Lloyd, D., 1990. A phenological classification of terrestrial vegetation cover using shortwave vegetation index imagery. *International Journal of Remote Sensing* 11, 2269–2279.
- Loik, M.E., Breshears, D.D., Lauenroth, W.K., Belpap, J., 2004. A multi-scale perspective of water pulses in dryland ecosystems: climatology and ecohydrology of the western USA. *Oecologia* 141 (2), 269–281.
- Mahmood, R., Hubbard, K.G., 2007. Relationship between soil moisture of near surface and multiple depths of the root zone under heterogeneous land uses and varying hydroclimatic conditions. *Hydrological Processes* 21 (25), 3449–3462.
- Martinez, C., Hancock, G.R., Kalma, J.D., Wells, T., 2008. Spatio-temporal distribution of near-surface and root zone soil moisture at the catchment scale. *Hydrological Processes* 22 (14), 2699–2714.

- Méndez-Barroso, L.A., 2009. Changes in Hydrological Conditions and Surface Fluxes due to Seasonal Vegetation Greening in North American Monsoon Region. M.S. Thesis. New Mexico Institute of Mining and Technology, Socorro, NM, 158 pp.
- Mohanty, B.P., Skaggs, T.H., Famiglietti, J.S., 2000. Analysis and mapping of field-scale soil moisture variability using high-resolution, ground-based data during the Southern Great Plains 1997 (SGP1997) hydrology experiment. *Water Resources Research* 36 (4), 1023–1031.
- Prasad, V.K., Anuradha, E., Badarinath, K.V.S., 2005. Climatic controls of vegetation vigor in four contrasting forest types of India. Evaluation from national oceanic and atmospheric administration's advanced very high resolution radiometer datasets (1990–2000). *International Journal of Biometeorology* 50 (1), 6–16.
- Reed, B.C., Brown, J.F., VanderZee, D., Loveland, T.R., Merchant, J.W., Ohlen, D.O., 1994. Measuring phenological variability from satellite imagery. *Journal of Vegetation Science* 5 (5), 703–714.
- Reynolds, J.F., Kemp, P.R., Ogle, K., Fernandez, R.J., 2004. Modifying the 'pulse-reserve' paradigm for deserts of North America: precipitation pulses, soil water, and plant responses. *Oecologia* 141 (2), 194–210.
- Salinas-Zavala, C.A., Douglas, A.V., Diaz, H.F., 2002. Interannual variability of NDVI in northwest Mexico: associated climatic mechanisms and ecological implications. *Remote Sensing of Environment* 82 (2–3), 417–430.
- Schenk, H.J., Jackson, R.B., 2002. The global biogeography of roots. *Ecological Monographs* 72 (3), 311–328.
- Sellers, P.J., 1985. Canopy reflectance, photosynthesis and transpiration. *International Journal of Remote Sensing* 6, 1335–1372.
- Seyfried, M.S., Murdock, M., 2004. Measurement of soil water content with a 50 MHz soil dielectric sensor. *Soil Science Society of America Journal* 68 (2), 394–403.
- Seyfried, M.S., Wilcox, B., 2006. Soil water storage and rooting depth: key factors controlling recharge on rangelands. *Hydrological Processes* 20, 3261–3275.
- Tucker, C.J., Townsend, J.R.G., Goff, T.E., 1985. African land cover classification using satellite data. *Science* 227, 369–375.
- Vachaud, G., Passerat De Silans, A., Balanis, P., Vauclin, M., 1985. Temporal stability of spatially measured soil water probability density function. *Journal of the Soil Society of America* 49, 822–828.
- Vivoni, E.R., Gutiérrez-Jurado, H.A., Aragón, C.A., Méndez-Barroso, L.A., Rinehart, A.J., Wyckoff, R.L., Rodríguez, J.C., Watts, C.J., Bolten, J.D., Lakshmi, V., Jackson, T.J., 2007. Variation of hydrometeorological conditions along a topographic transect in northwestern Mexico during the North American monsoon. *Journal of Climate* 20 (9), 1792–1809.
- Vivoni, E.R., Gebremichael, M., Watts, J.C., Bindlish, R., Jackson, T.J., 2008a. Comparison of ground-based and remotely-sensed surface soil moisture estimates over complex terrain during SMEX04. *Remote Sensing of Environment* 112 (2), 314–325.
- Vivoni, E.R., Moreno, H.A., Mascaró, G., Rodríguez, J.C., Watts, C.J., Garatuza-Payan, J., Scott, R.L., 2008b. Observed relation between evapotranspiration and soil moisture in the North American Monsoon region. *Geophysical Research Letters* 35, L22403. doi:10.1029/2008GL036001.
- Wang, J., Rich, P.M., Price, K.P., 2003. Temporal responses of NDVI to precipitation and temperature in the central Great Plains, USA. *International Journal of Remote Sensing* 24 (11), 2345–2364.
- Wang, W., Anderson, T.B., Phillips, N., Kaufman, K.R., Potter, C., Myneni, B.R., 2006. Feedbacks of vegetation on summertime climate variability over the North American Grasslands. Part I: statistical analysis. *Earth Interactions* 10 (17), 1–27.
- Watts, C.J., Scott, R.L., Garatuza-Payan, J., Rodríguez, J.C., Prueger, J.H., Kustas, W.P., Douglas, M., 2007. Changes in vegetation condition and surface fluxes during NAME 2004. *Journal of Climate* 20 (9), 1810–1820.
- Weiss, J.L., Gutzler, D.S., Coonrod, J.E.A., Dahm, C.N., 2004. Seasonal and inter-annual relations between vegetation and climate in central New Mexico, USA. *Journal of Arid Environments* 57 (4), 507–534.
- Xinmei, H., Lyons, T.J., Smith, R.C.G., Hacker, J.M., Schwerdtfeger, P., 1993. Estimation of surface energy balance from radiance surface temperature and NOAA-AVHRR sensor reflectances over agricultural and native vegetation. *Journal of Applied Meteorology* 32 (8), 1441–1449.
- Zhang, X., Friedl, M.A., Schaaf, C.B., Strahler, A.H., Hodges, J.C.F., Gao, F., Reed, B.C., Huete, A., 2003. Monitoring vegetation phenology using MODIS. *Remote Sensing of Environment* 84 (3), 471–475.
- Zhu, C.M., Cavazos, T., Lettenmaier, D.P., 2007. Role of antecedent land surface conditions in warm season precipitation over northwestern Mexico. *Journal of Climate* 20 (9), 1774–1791.